Supporting information

Influence of mixing in coprecipitation on structural evolution of Cu-Zr catalysts

Xin Jiang*[a,b], Bing Han[a], Ying Zhuang[a]

([a]*College of Chemical and Biological Engineering, Zhejiang University, Hangzhou* 310027*, P. R. China*

[b] *Zhejiang Provincial Key Laboratory of Advanced Chemical Engineering Manufacture Technology, Zhejiang University, Hangzhou 310058, P. R. China*)

Corresponding author: Xin Jiang, E-mail address: jiangx@zju.edu.cn

1. Experimental Methods

Figure 1 shows a schematic diagram of the stirred tank reactor setup. The detailed procedure for catalyst preparation in the stirred tank is as follows. A mixed salt solution of $Cu(NO_3)_2$ and $Zr(NO_3)_4$ with a Zr^{4+} molar ratio of 10% ($Zr^{4+}/(Cu^{2+}+ Zr^{4+})$) and a total concentration of 0.1 mol/L was prepared, along with a 0.1 mol/L Na_2CO_3 solution. Using a dual-channel syringe pump, the mixed salt solution and Na_2CO_3 solution were simultaneously injected into a beaker placed in an ice-bath thermostatic magnetic stirrer. The flow rates of the mixed salt solution and Na_2CO_3 solution were controlled at 255 mL/h and 348 mL/h, respectively, to maintain the reaction pH between 6.8 and 7.0.

After reaction, the precipitated product was centrifuged, washed, and filtered, followed by drying in an oven at 100 ℃ for 18 h to obtain the precipitate. The dried precipitate was then calcined at 350 ℃ for 3 h to form the oxide. Finally, the oxide was sieved to obtain particles with a size range of 0.25-0.38 mm. These oxide particles were reduced under H_2 atmosphere at 300 ℃ for 2 h to yield the Cu-Zr catalyst.

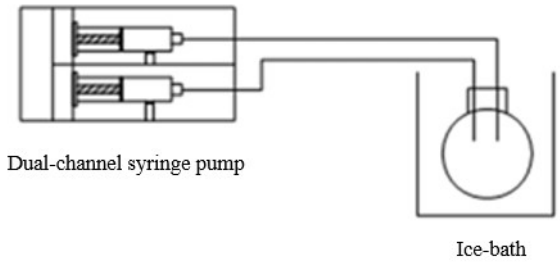

Figure S1. Diagram of catalyst preparation process in the stirred tank reactor

2. Results and Discussion

Figure S2 shows the effect of aging time on the methanol synthesis performance of Cu-Zr catalysts. As can be observed, both methanol selectivity and CO_2 conversion rate significantly decrease with prolonged aging time,

indicating that the non-aged catalyst exhibits superior catalytic performance. Therefore, in this study, we directly calcined the non-aged precipitate to prepare the catalyst and investigated the influence of mixing on the structural evolution of the catalyst.

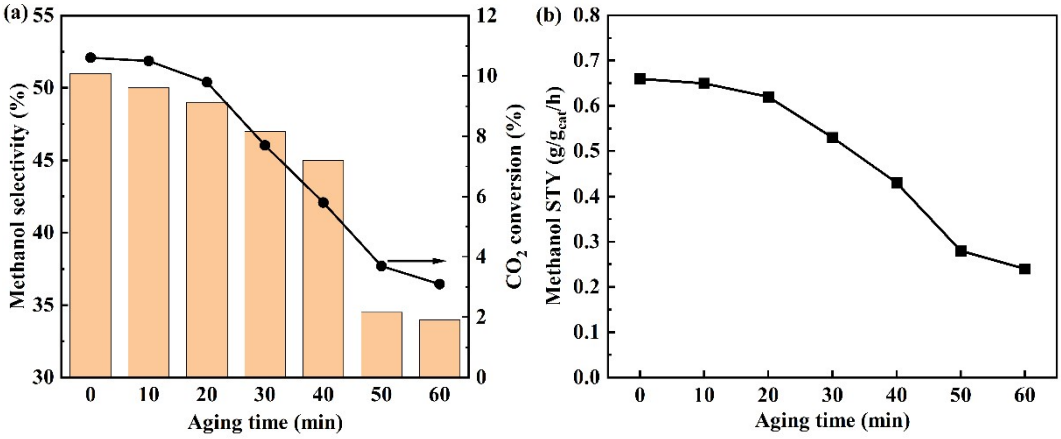

Figure S2. The effect of aging time on catalytic performance of Cu-Zr catalysts for CO_2 hydrogenation to methanol: (a) CO_2 conversion (240 ℃) and methanol selectivity (at 10% CO_2 conversion), and (b) methanol STY (240 ℃)

Figure S3 shows the XRD patterns of the non-aged Cu-Zr precipitates. As can be seen, the XRD patterns of precipitates prepared at flow rates of 10 mL/min and 60 mL/min show no distinct diffraction peaks, indicating that precipitates exhibit an amorphous structure.

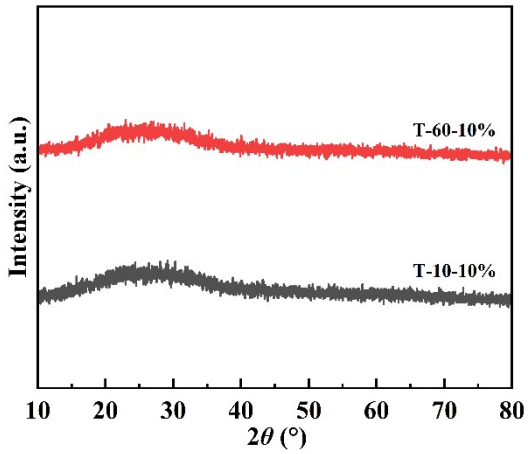

Figure S3. XRD patterns of Cu-Zr precipitates

Figure S4 presents TEM images with EDS elemental mapping of the oxide samples. The analysis clearly reveals distinct Zr-rich and Cu-rich domains in the low flow rate sample, while the high flow rate sample shows homogeneous distribution of both Cu and Zr elements without noticeable enrichment regions. Cross-referencing with the TEM results of precipitates, we conclude that the observed non-uniform elemental distribution in oxides stems from the initial structural heterogeneity of the precipitates. During thermal decomposition, Cu-rich regions preferentially form isolated copper oxide particles, while Zr-rich regions develop separate zirconia particles. As a result, the spatial distribution heterogeneity of Cu and Zr in the precipitates is preserved in the calcined oxide

structure.

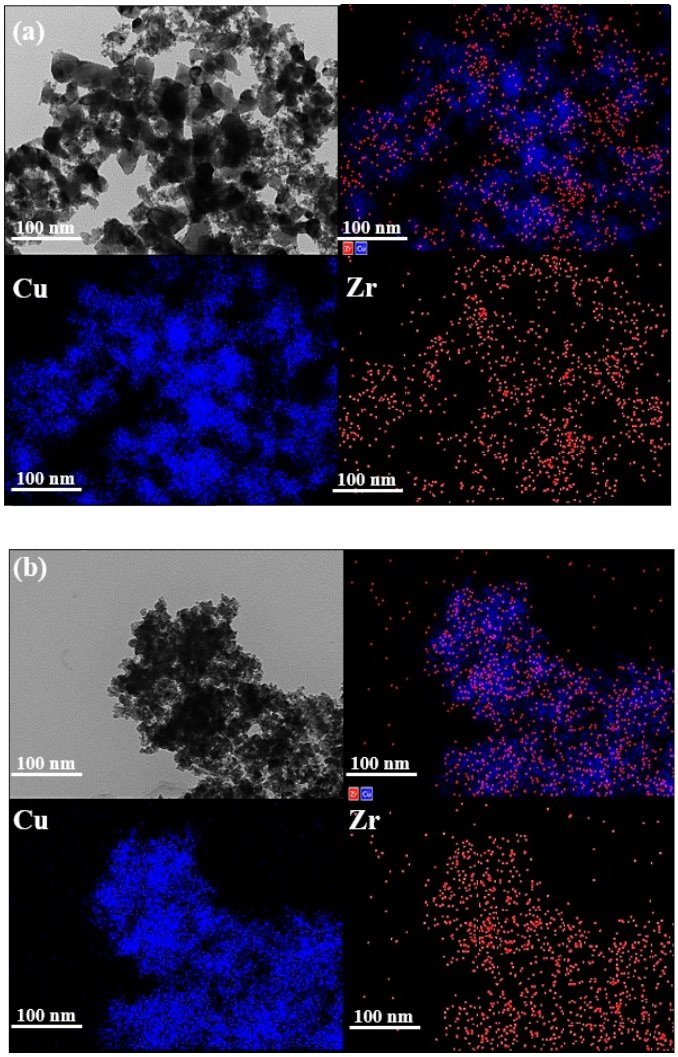

Figure S4. TEM-EDS mapping images of Cu-Zr oxides (10%Zr): (a) 10 mL/min, and (b) 60 mL/min

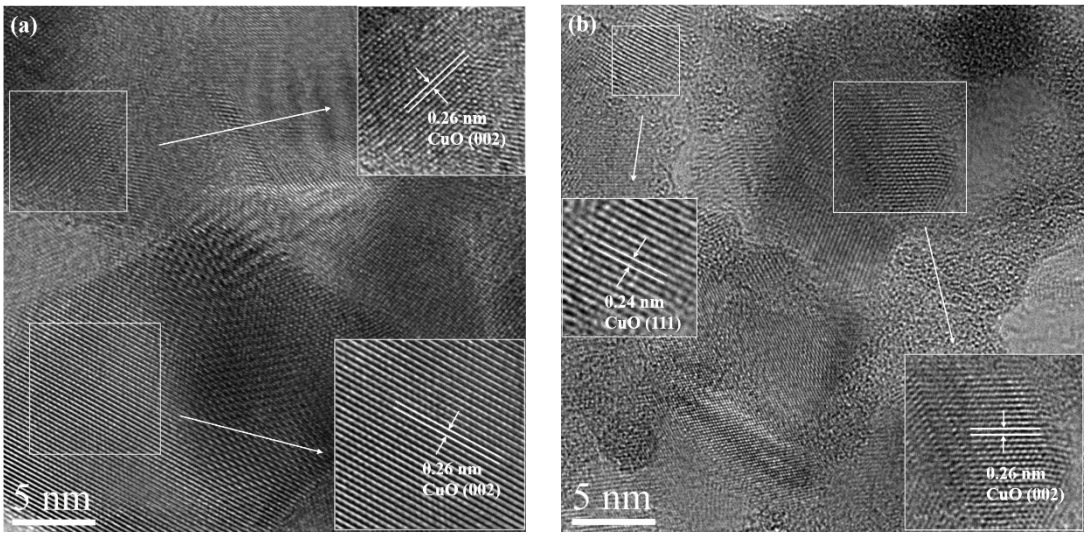

Figure S5. HRTEM images of Cu-Zr oxides (10%Zr): (a) 10 mL/min, and (b) 60 mL/min

Figure S5 shows HRTEM images of the oxide samples. TEM analysis clearly reveals lattice fringes corresponding to crystalline CuO in both oxide samples, while no lattice structures associated with ZrO_2 are observed, confirming the amorphous nature of zirconia in these oxides.

Figure S6 shows the methanol STY comparison of Cu-Zr catalysts prepared at flow rates of 10 mL/min and 60 mL/min. At 60 mL/min, the methanol STY first increases rapidly with Zr content and then slightly decreases, reaching its maximum at 10% Zr content. This is because, At 60 mL/min, the Cu-Zr interface increases significantly at 10% Zr, while further increasing Zr content does not lead to noticeable changes in the Cu-Zr interface. In contrast, at 10 mL/min, the methanol yield rises slowly and continuously with increasing Zr content, peaking at 30% Zr, which correlates with the gradual increase in the Cu-Zr interface. Comparing the two flow rates, the methanol yield is significantly higher at 60 mL/min than at 10 mL/min for the same Zr content, benefiting from the greater Cu-Zr interfacial sites formed under faster flow conditions. Additionally, the T-60-10% catalyst demonstrates comparable methanol STY to industrial Cu-Zn-Al catalysts, confirming the superiority of microreactors in optimizing Cu-Zr catalyst structure and enhancing catalytic performance.

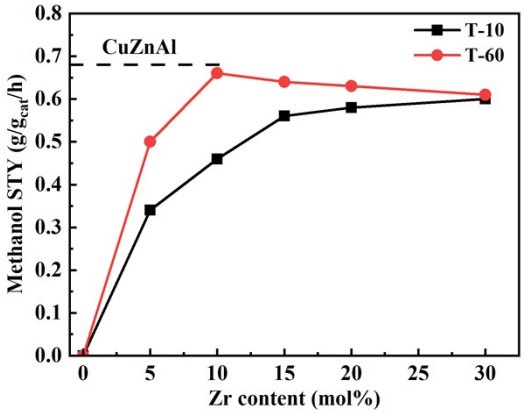

Figure S6. Methanol STY of Cu-Zr catalysts prepared at 10 mL/min and 60 mL/min